



1 Article

2 Retinal Blood Velocity and Flow in Early Diabetes 3 and Diabetic Retinopathy Using Adaptive Optics 4 Scanning Laser Ophthalmoscopy

5 Cherilyn Mae A. Palochak^{1,2}, Hee Eun Lee¹, Jessica Song¹, Andrew Geng¹, Robert A.
6 Linsenmeier³, Stephen A. Burns⁴, Amani A. Fawzi¹

7 ¹ Department of Ophthalmology, Feinberg School of Medicine, Northwestern University, Chicago, IL 60611
8 USA

9 ² Chicago Medical School, Rosalind Franklin University of Medicine and Science, North Chicago, IL 60064,
10 USA

11 ³ Department of Biomedical Engineering, Northwestern University, Evanston, IL 60208, USA

12 ⁴ School of Optometry, Indiana University, Bloomington, IN 47405, USA

13 * Correspondence: afawzim@gmail.com; Tel.: +1 (312) 908-8152; Fax: +1 (312) 503-8152

14 Received: date; Accepted: date; Published: date

15 **Abstract:** Using Adaptive Optics Scanning Laser Ophthalmoscopy (AOSLO), we measured retinal
16 blood velocity and flow in healthy control eyes and eyes of diabetic patients with or without
17 retinopathy. This cross-sectional study included 39 eyes of 30 patients with diabetes (DM) with mild
18 non-proliferative diabetic retinopathy (NPDR) or without retinopathy (DM no DR) and 21 eyes of
19 17 healthy age-matched controls. Participants were imaged with a commercial OCTA device
20 (RTVue-XR Avanti) and AOSLO device (Apaeros Retinal Imaging System, Boston Micromachines).
21 We analyzed AOSLO-based retinal blood velocity and flow, and OCTA-based vessel density of the
22 superficial (SCP), deep retinal capillary plexus (DCP) and full retina. Retinal blood velocity was
23 significantly higher in eyes with DM no DR and lower in NPDR across all vessel diameters
24 compared to controls. Retinal blood flow was significantly higher in DM no DR and lower in NPDR
25 in vessel diameters up to 60µm compared to controls. When comparing flow outliers (low flow DM
26 no DR eyes and high flow NPDR eyes), we found they had a significantly different retinal vessel
27 density compared to the remaining eyes in the respective groups. Retinal blood velocity and flow is
28 increased in eyes with DM no DR, while these parameters are decreased in eyes with mild NPDR
29 compared to healthy age-matched controls. The similarity of OCTA vessel density among outliers
30 in the two diabetic groups suggests an initial increase followed by progressive decline in blood flow
31 and OCTA vessel density with progression to clinical retinopathy, which warrants further
32 investigation.

33 **Keywords:** adaptive optics scanning laser ophthalmoscopy, optical coherence tomography
34 angiography, diabetic retinopathy, diabetes mellitus, retina, blood flow
35

36 1. Introduction

37 Diabetic retinopathy (DR) is a microvascular complication affecting 35% of patients with
38 diabetes, and is the leading cause of preventable blindness in working age adults worldwide [1-3].
39 DR is associated with hemorheological and vascular changes that lead to impaired autoregulation
40 early on in the disease followed by progressive attenuation of the retinal microcirculation, with the
41 clinical outcome being retinal ischemia and angiogenesis [4]. Given that retinal vascular dysfunction
42 is central to its pathophysiology, a large body of research has focused on retinal blood flow in DR [5-
43 7]. These studies, however, have generated a great deal of controversy, particularly regarding the

44 direction of change of retinal blood flow in the early stages prior to the onset of clinical manifestations
45 of DR [8,9].

46 Studies using fluorescein angiography with videography (VFA) relied on the mean transit time
47 to estimate retinal blood flow. While some of these studies found increasing blood flow with
48 worsening DR [5,9,10], others reported initial decreased flow in diabetic eyes without DR followed
49 by increased flow with the onset of non-proliferative diabetic retinopathy (NPDR) [11,12]. Laser
50 Doppler techniques measure single vessel velocity and diameter to estimate retinal blood flow. Most
51 Doppler studies reported increased diameters and decreased velocity in diabetic subjects with and
52 without DR, yet their blood flow reports were conflicting [13-19]. Some reported increased flow in
53 DM with no DR or NPDR compared to controls [13-15,20], others reported increased flow in NPDR
54 but no change in DM with no DR [18], and others no significant flow change in either [16]. Color
55 Doppler imaging (CDI) studies based on ultrasound measured the larger vessels at the optic nerve
56 and similarly reported mixed results for the impact of diabetes on blood flow velocity [21-24].
57 Limitations of these techniques must be considered to attempt to resolve these conflicting findings.
58 VFA, CDI, and Laser Doppler deduce total retinal flow indirectly from single vessel measurements.
59 These techniques generally focus on vessels larger than 50 μ m, and none of them are able to measure
60 capillary flow. Modern techniques to image retinal vasculature include Doppler optical coherence
61 tomography (OCT) and adaptive optics (AO) ophthalmoscopy. Doppler OCT offers non-invasive, *in*
62 *vivo* assessment of all the major peripapillary retinal venous diameters and their blood velocity and
63 thus measures the absolute total retinal blood flow from an eye [25,26]. Using this technology,
64 researchers showed that retinal blood flow is significantly decreased in eyes with severe NPDR and
65 PDR compared to controls [27-29]. Notably however, Doppler OCT focuses on measuring all large
66 peripapillary vessels and does not specifically capture small caliber vessels in the parafoveal region.

67 In contrast to previous imaging modalities which typically examined larger vessels, AO
68 scanning laser ophthalmoscopy (AOSLO) allows imaging of blood velocity and flow across a wider
69 range of vessel diameters [30-32]. Techniques to study the retinal microvasculature with AOSLO
70 include high frame rate non-confocal imaging [33,34], single scan lines of a vessel (XT imaging)
71 [35,36], and dual-channel scanning [37]. High frame rate non-confocal imaging and dual-channel
72 scanning can measure flow velocity in capillaries <15 μ m. The XT imaging AOSLO technique
73 introduced by Zhong et al. measures velocity and flow in medium to large sized vessels (15–100 μ m)
74 [35].

75 In this study, we used AOSLO XT imaging to study the hemodynamic changes in medium (15–
76 60 μ m) to large-sized retinal vessels (60–100 μ m) in patients who have DM without DR and those with
77 mild NPDR to resolve the controversy regarding retinal blood flow changes in the early stages of
78 diabetes. We compared the vessel diameter, blood velocity and volumetric flow in the retinal
79 vasculature in diabetic subjects to those in age-matched controls and studied the parafoveal capillary
80 density in these subjects using OCT angiography.

81 2. Methods

82 2.1 Study Design and Human Subjects

83 Patients were recruited in the Department of Ophthalmology at Northwestern University in
84 Chicago, Illinois between July 2018 and March 2019. The study was approved by the Institutional
85 Review Board of Northwestern University, followed the tenets of the Declaration of Helsinki, and
86 was in accordance with the Health Insurance Portability and Accountability Act regulations. Written
87 informed consent was obtained from all patients before image acquisition.

88 Inclusion criteria were healthy subjects, and subjects with diabetes and eyes with DM without
89 DR or mild NPDR based on clinical assessment by board certified ophthalmologists. Inclusion criteria
90 for healthy eyes included no history of ophthalmic disease confirmed by clinical examination. Eyes
91 of subjects with diabetes with or without mild NPDR were included based on clinical exam and
92 patient history, including no evidence of prior ocular therapeutic intervention for diabetes (e.g.
93 surgery, intravitreal injection, or pan-retinal photocoagulation). Classification of eyes with mild

94 NPDR were graded based on the range of the Early Treatment for Diabetic Retinopathy Study
95 (ETDRS) scale [38,39]. Type 1 and type 2 diabetics were included.

96 Eyes were excluded from the study if they had evidence of other ocular disorders (e.g. cataract,
97 glaucoma, age-related macular degeneration). We excluded eyes with cataract graded above nuclear
98 opalescence grade three or nuclear color grade three that may compromise image quality. We also
99 excluded poor quality AOSLO images and optical coherence tomography angiography (OCTA)
100 images with quality scores ≤ 5 and signal strength index (SSI) < 60 .

101 Electronic medical records were reviewed to extract demographic and clinical information. All
102 patients underwent a dilated eye exam and axial length measurements through optical biometry at
103 the same visit. All measurements were conducted by a single certified examiner using an IOLMaster
104 700 (ZEISS, Jena, Germany).

105 2.2 Optical Coherence Tomography Angiography (OCTA)

106 OCTA images of $3 \times 3 \text{ mm}^2$ centered on the fovea were acquired using the RTVue-XR Avanti
107 system (Optovue Inc., Fremont, California) with split-spectrum amplitude-decorrelation angiography
108 (SSADA) software [40]. SSADA detects flow by quantifying decorrelation of OCT reflectance between
109 two consecutive B-scans at the same location on the retina. The specifications of the machine include an
110 A-scan rate of 70,000 scans per second, a light source centered on 840 nm, and a bandwidth of 45 nm.
111 *En face* OCT angiograms were used as a map to guide AOSLO imaging and to identify vessels of interest
112 within the superficial retinal vasculature. We used the periarterial capillary-free zone to distinguish
113 arteries from veins [41]. Parameters regarding vessels of interest are further explained under the
114 AOSLO XT imaging methods section.

115 We then used the built-in AngioVue Analytics software (version 2017.1.0.151) to quantify the
116 “parafoveal” vessel density of the superficial capillary plexus (SCP), deep capillary plexus (DCP), and
117 full retina. The “parafovea” was defined as an annulus centered on the fovea with inner and outer ring
118 diameters of 1 mm and 3 mm, respectively. Vessel density was defined as the area occupied by vessels
119 and microvasculature and is reported as a percentage of the total area.

120 2.3 Adaptive Optics Scanning Laser Ophthalmoscopy (AOSLO)

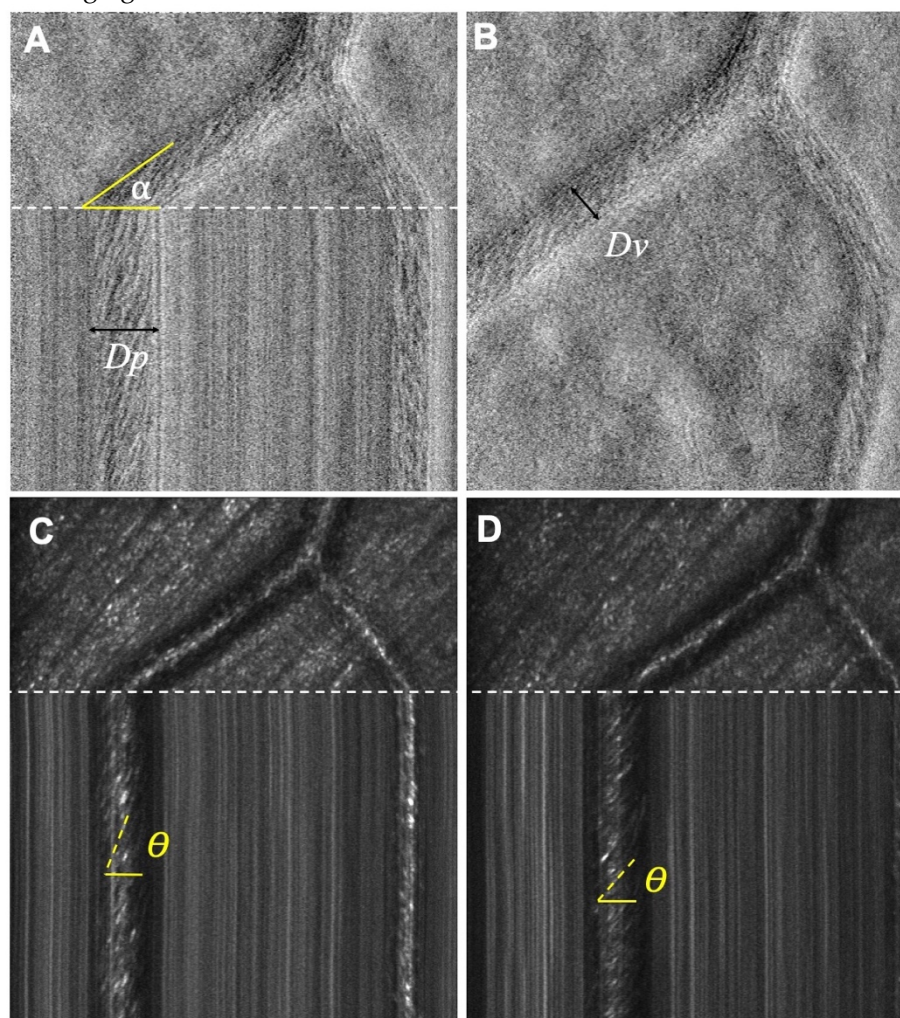
121 AOSLO imaging was done using the Apalios Retinal Imaging System (Boston Micromachines
122 Corporation, Cambridge, Massachusetts) [42]. It uses a 97 actuator ALPAO DM (ALPAO SAS,
123 Montbonnot, France) with $25 \mu\text{m}$ of stroke for wavefront correction, and two superluminescent diodes
124 (SLD) as light sources centered at 790 and 850 nm with respective bandwidths of 15 and 20 nm. Imaging
125 was performed using the 790 nm source and wavefront sensing was performed using the 850 nm
126 source, with a combined power at the eye of approximately $130 \mu\text{W}$. Split-detection images were also
127 acquired using two separate non-confocal detectors. Image intensity was determined by the difference
128 of the non-confocal detector signals divided by their sum.

129 We acquired *en face* images of $1.5^\circ \times 1.77^\circ$ dimension focused on vessels. We focused the machine
130 at the center of the lumen in vessels of interest and acquired multiple 2 second videos of 60 frames (30
131 frames/second) to ensure inclusion of flow variations throughout the cardiac cycle.

132 2.4 AOSLO XT imaging

133 To measure blood velocity and flow, we employed XT imaging as described by Zhong et al. [35,36].
134 Vessels of interest, either arteries or veins, were identified from the relevant $3 \times 3 \text{ mm}^2$ OCTA image
135 centered on the fovea. The ultimate goal in XT imaging was to obtain pictures with well-delineated
136 vessel walls and clear streaks focused on the center of the vessel lumen. Briefly, the default mode of
137 scanning in the AOSLO uses a horizontal scanner that moves down vertically during image acquisition.
138 As the scanner moves down, lines of information are taken in succession and stitched together to form
139 a full 2-dimensional image in the frontal plane of the retina—this type of image is referred to as an XY
140 image. In an XT image, the vertical scanner is halted momentarily at a point of interest and takes lines
141 of images sequentially at the same location. While XY images have two spatial dimensions, the two axes

142 of the frontal plane, XT images have one spatial dimension (horizontal) and one temporal dimension
 143 (acquisition sequence). In practice we obtain video frames which are split between XY images (**Figure**
 144 **1, B**) and XT (**Figure 1, bottom**). This dual mode video frame simplifies detection of eye movements
 145 by comparing the XY portion of sequential video frames. When properly focused on the vessel lumen,
 146 XT images will produce diagonal streaks (**Figure 1**) which represent erythrocyte flow. Using the slopes
 147 of the erythrocytes on the XT portion of our images, we can then extract the spatial and temporal
 148 information to calculate the velocity of these cells. While temporal information can be measured
 149 between successive XY images, the frame rate used (30 Hz) is too limited to track individual blood cells
 150 in the medium to large-sized vessels (15 – 105 μm diameter) vessels we targeted. This limitation is
 151 overcome by XT imaging, which uses a 15kHz horizontal line rate.



152
 153 **Figure 1.** AOSLO Split-detector and Confocal Images. (A) Single frame split-detector images showing XT
 154 image with the scan intersecting the blood vessel at angle alpha. The vessel lumen width was determined
 155 from the XT scan (Dp). (B) XY image showing the direct diameter of the vessel (Dv). (C, D) AOSLO confocal
 156 images showing the theta angle of RBC slopes at different phases of the cardiac cycle. Shallower slopes
 157 indicate higher velocity.

158 Several intrinsic qualities of the vessels ensured high accuracy measures of erythrocyte velocity
 159 and were set as criteria for vessels of interest. These are the (1) alpha angle, (2) distance from
 160 bifurcations, and (3) vessel size. The alpha angle influences accuracy because the scanner is fixed and
 161 does not have rotating capabilities. An alpha angle between $50\text{--}90^\circ$ causes two things to occur: the
 162 horizontal component of velocity (Vp) is too small along the X-axis, and the horizontal distance traveled
 163 by particles (Dp) decreases, thus decreasing the size of the streak. Both of these factors contribute to
 164 increased uncertainty in the horizontal component of blood velocity and were therefore avoided.
 165 Secondly, the smaller the vessel size, the more difficult it is to center on the lumen, in the presence of

166 small eye movements, resulting in poor visualization and fewer streaks. Thus, we focused on medium
 167 sized vessels larger than 15 μm in diameter. Lastly, we avoided measuring too close to bifurcations to
 168 avoid uneven flow distributions across the vessel, which affects the velocity and flow [35].

169 2.5 XT imaging analysis: Blood Velocity and Flow Calculations

170 Flow and velocity measurements were completed by three independent graders (CAP, HEL, and
 171 JS). Two of the graders were masked to the health status of the eye to remove bias. Image quality was
 172 determined by the lack of ocular movement (stationary structures presented as straight vertical lines)
 173 and streak contrast and clarity. We then followed the protocol set forth by Zhong et al., with a few
 174 adaptations. Briefly, to calculate the velocity of erythrocytes in the lumen, the slopes of the streaks in
 175 the confocal XT image were measured using angle θ ($0 < \theta < \pi/2$) against the horizontal line (**Figure 1**).
 176 Based on this slope, the horizontal vector of velocity (V_p) is given by:

$$V_p = \frac{f \cdot \cot\theta}{k} \quad (1)$$

177 where f is the horizontal frame rate (15kHz) to calibrate for time, and k is the calculated magnification
 178 taking into account the axial length. The velocity within the axis of the vessel is then:

$$V_{ax} = \frac{V_p}{\cos\alpha} \quad (2)$$

179 To calculate flow, we measured the diameter of the lumen and alpha angle on the split-detector
 180 images, which differed from Zhong's protocol. The use of split-detector images (versus confocal)
 181 allowed better visualization of the inner and outer vessel walls. Vessel lumen diameter (D_v) was
 182 calculated using the measured alpha angle and the horizontal distance of the XT image (D_p) based on
 183 equation 3. The measurement was confirmed by directly measuring the vessel lumen diameter in the
 184 XY image (**Figure 1**). Given the lumen diameter and velocity, blood flow (Q) was calculated based on
 185 equation 4.

$$D_v = D_p \cdot \sin\alpha \quad (3)$$

$$Q = \frac{V_{ax} \cdot \pi \cdot D_v^2}{4} \quad (4)$$

186 In selecting XT images, we sought to minimize factors that could artificially change flow and
 187 velocity such as ocular movement. In the XT portion of the images, static structures should appear as
 188 straight lines. Any deviations indicate small ocular movements and these images were discarded from
 189 the analysis. We used at least three particle streaks centered in the lumen with the shallowest slopes to
 190 measure the average maximum velocity. In order to account for the variations of velocity and flow due
 191 to pulsation, we selected images with either maximum or minimum RBC slopes from multiple
 192 image sequences taken at the same location and categorized them into two sets of images (minimum
 193 vs. maximum, 2-4 images each). We used the average of the minimum and maximum calculated
 194 velocities from these two sets of non-sequential frames in order to determine the average velocity for
 195 each vessel. All images were exported and measured on ImageJ (developed by Wayne Rasband,
 196 National Institutes of Health [NIH], Bethesda, MD, USA; available in the public domain at
 197 <http://rsb.info.nih.gov/ij/index.html>).

198 2.6 Statistical Analysis

199 Statistical analysis was performed using IBM SPSS software version 25 (IBM SPSS Statistics; IBM
 200 Corporation, Chicago, IL, USA) with the significance level set at 0.05. Descriptive statistics were
 201 calculated for all groups, and variables were expressed as mean \pm standard deviation (SD).

202 Characteristics of the study population were compared by independent *t*-test for continuous
 203 parameters and by chi-square test for categorical parameters. Pearson correlations were performed to
 204 determine the correlation between velocity and diameter of each group, and to determine whether the
 205 degree of correlation differed across the groups. One-way analysis of variance (ANOVA) was used to
 206 compare the difference between all groups. Populations were tested for equality of variance using the
 207 Levene test for homogeneity of variances. If the distributions failed, then Welch ANOVA was
 208 performed to correct for inhomogeneity of variances. Tukey or Games-Howell post-hoc tests were
 209 performed following one-way or Welch ANOVA, respectively. The main outcome measures were
 210 vessel diameter, blood velocity and flow.

211 **3. Results**

212 *3.1 Subjects*

213 The overall demographic, clinical and disease-related characteristics are reported in **Table 1**. Of
 214 the 65 eyes that were imaged for this study, 5 were excluded due to motion artifact on XT images,
 215 leaving a total of 60 eyes from 47 participants (30 diabetic, 17 healthy controls). There were no
 216 significant differences in age or gender between groups. There were no significant differences in
 217 diabetes type, disease duration, and hemoglobin A1c (HbA1c) between subjects with diabetes with
 218 and without mild NPDR. Additional demographics and disease related characteristics are reported
 219 in **Table 1**.

220 **Table 1.** Patient Demographics, Clinical and Diabetes Characteristics and Capillary Measurements on
 221 Optical Coherence Tomography Angiography

	Healthy Controls	DM no DR	NPDR	P
Patients, n	17	21	9	
Eyes, n	21	26	13	
Vessel segments, n	94	110	56	
Vessel diameter range (µm)	15.98–97.93	18.27–91.88	32.71–99.45	
Age, mean ± SD, range	57.7 ± 11.5 29–74	49.1 ± 16.3 19–71	47.6 ± 13.6 32–69	0.119
Sex				0.069
Female, n (%)	13 (76%)	10 (48%)	3 (33%)	
Male, n (%)	4 (23%)	11 (52%)	6 (66%)	
DM type				0.398*
Type 1, n (%)	n/a	6 (29%)	4 (44%)	
Type 2, n (%)	n/a	15 (71%)	5 (56%)	
Disease duration, y, mean ± SD	n/a	9.3 ± 7.6	15.2 ± 8.5	0.070*
HbA1c, mean ± SD	n/a	7.3 ± 1.9	7.3 ± 1.1	0.998*
Lens status				0.943
Clear	8 (47%)	11 (52%)	5 (56%)	
Cataract	8 (47%)	9 (43%)	3 (33%)	
Pseudophakic	1 (6%)	1 (5%)	1 (11%)	
Hypertension, n (%)	1 (6%)	9 (43%)	3 (33%)	–
Parafoveal vessel density (%)				
SCP, mean ± SD	47.97 ± 3.95	45.15 ± 4.49	43.23 ± 3.80	0.010
DCP, mean ± SD	53.57 ± 3.19	50.12 ± 3.50	47.59 ± 3.86	0.000
Full retina, mean ± SD	57.69 ± 3.35	55.55 ± 3.80	54.25 ± 2.67	0.023
OCTA SSI, mean ± SD	68.85 ± 6.15	67.45 ± 4.24	69.55 ± 6.62	0.522

222 Abbreviations: DM = diabetes mellitus, DR = diabetic retinopathy, NPDR = non-proliferative diabetic
 223 retinopathy, SCP = superficial capillary plexus, DCP = deep capillary plexus, SD = standard deviation. *P*-value

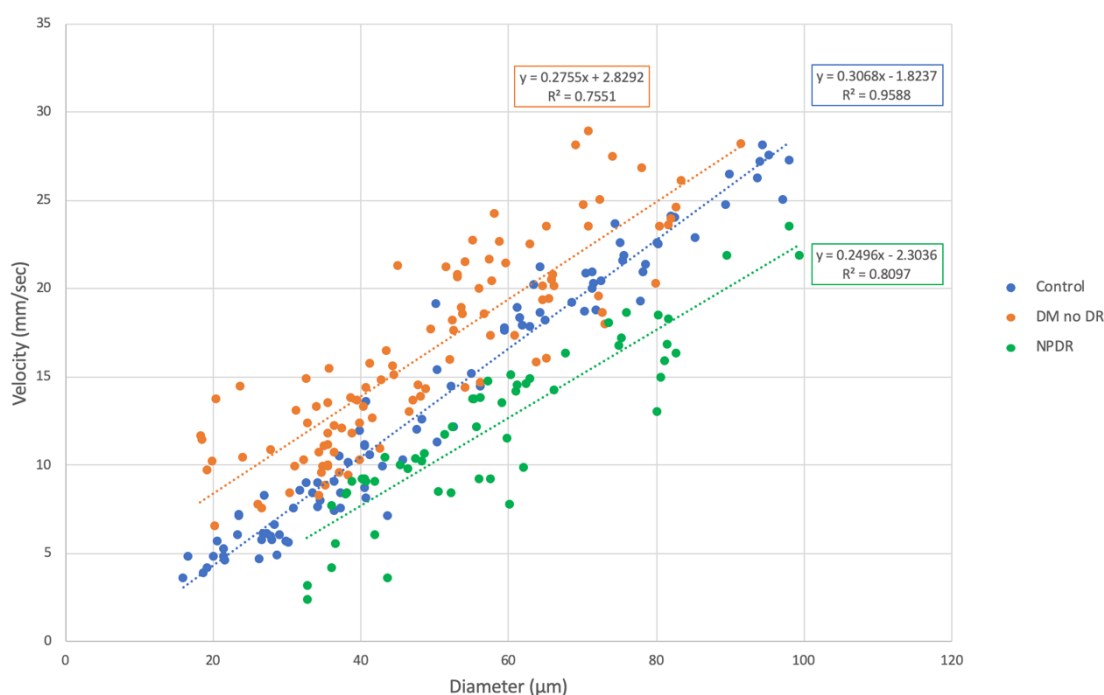
224 represents one-way ANOVA between all three groups. *P-value represents independent t-test or Chi-square test
 225 between DM without DR and NPDR. The healthy controls were not included.

226 3.2 OCTA Parafoveal Vessel Density

227 OCTA parafoveal densities of the SCP, DCP, and full retina were significantly different between
 228 the groups. The overall results are reported in **Table 1**.

229 3.3 Comparison of AOSLO blood velocity across groups

230 As expected, we found a significant correlation between mean velocity and diameter in all
 231 groups, where velocity increased with increasing diameter (**Figure 2**). This trend was found to be
 232 true in arteries and veins. Linear regression coefficients (r) were 0.979 for controls, 0.880 for DM
 233 without DR and 0.900 for NPDR eyes. One-way ANOVA comparing the regression coefficients
 234 showed a significant difference between the three groups (P=0.007). One-way ANOVA showed a
 235 statistically significant difference in velocity across all vessel diameters comparing all three groups
 236 (**Table 2**). Eyes with DM without DR had significantly higher velocity than control vessels up to 60µm
 237 and higher than NPDR for all diameters. NPDR eyes had velocities significantly lower than controls
 238 and DM no DR eyes across all vessel diameters (**Table 2**). When we examined these differences by
 239 arterioles and venules, we found that eyes with DM without DR had significantly higher velocity
 240 than controls arteries up to 60µm and veins up to 30µm (**Table 3** and **Table 4**). Eyes with DM without
 241 DR had significantly higher velocity than NPDR across all arterial and venous diameters. NPDR eyes
 242 had velocities significantly lower than controls especially in arteries >60µm and veins >50µm.



243

244 **Figure 2.** Blood Velocity in Retinal Vessels (Arterioles, Venules and Capillaries) by Vessel Diameter,
 245 Comparing Healthy Controls, Diabetes without Retinopathy, and Non-proliferative Diabetic
 246 Retinopathy. A significant correlation was observed between velocity and vessel diameter in both
 247 arteries and veins within groups. Linear regression coefficients (r) were 0.979 for controls, 0.880 for
 248 DM without DR and 0.900 for NPDR eyes. One-way ANOVA comparing regression coefficients
 249 showed a significant difference across the three groups (P=0.007). Abbreviations: DM = diabetes
 250 mellitus, DR = diabetic retinopathy, NPDR = non-proliferative diabetic retinopathy.

251 **Table 2.** Summary of Blood Velocity in Arterioles and Venules by Vessel Diameter Groups,
 252 Comparing Healthy Controls, Diabetes without Retinopathy, and Non-proliferative Diabetic
 253 Retinopathy

	Control mm/sec (n=94)	DM no DR mm/sec (n=110)	NPDR mm/sec (n=56)	ANOVA P	Control vs DM no DR P	Control vs NPDR P	DM no DR vs NPDR P
< 30µm (n=34)	3.60–8.32, 5.59 (23)	6.54–14.49, 10.42 (11)	n/a	0.000			
31–40µm (n=62)	5.64–13.58, 9.08 (20)	8.29–15.47, 11.51 (31)	2.42–9.23, 6.68 (11)	0.000	0.000	0.020	0.000
41–60µm (n=75)	7.13–19.18, 13.35 (15)	10.95–24.28, 17.67 (36)	3.59–15.13, 10.66 (24)	0.000	0.000	0.032	0.000
> 61 (n=89)	17.84–28.15, 21.98 (36)	15.88–28.94, 22.88 (32)	9.85–23.54, 16.70 (21)	0.000	0.499	0.000	0.000

254 Blood velocity, expressed as range in mm/sec, mean (n), comparing different vessel diameters across groups. N
 255 equals number of measured vessel segments. P values were obtained using ANOVA and post-hoc tests.
 256 Abbreviations: DM = diabetes mellitus, DR = diabetic retinopathy, NPDR = non-proliferative diabetic
 257 retinopathy.

258 **Table 3.** Summary of Arteriolar Blood Velocity by Vessel Diameter Groups, Comparing Healthy
 259 Controls, Diabetes without Retinopathy, and Non-proliferative Diabetic Retinopathy

	Control mm/sec (n=55)	DM no DR mm/sec (n=79)	NPDR mm/sec (n=47)	ANOVA P	Control vs DM no DR P	Control vs NPDR P	DM no DR vs NPDR P
< 30µm (n=13)	4.22–7.15, 5.51 (9)	6.54–14.49, 10.59 (4)	n/a	0.001			
31–40µm (n=34)	7.98–11.14, 9.42 (9)	9.41–15.47, 12.07 (18)	2.42–9.23, 7.17 (7)	0.000	0.000	0.169	0.006
41–60µm (n=57)	10.33–19.18, 14.10 (9)	12.69–24.28, 18.02 (28)	6.06–15.13, 11.34 (20)	0.000	0.025	0.113	0.000
> 60µm (n=77)	17.84–28.15, 22.43 (28)	16.06–28.94, 22.98 (29)	9.85–23.54, 16.82 (20)	0.000	0.801	0.000	0.000

260 Blood velocity, expressed as range in mm/sec, mean (n), comparing different arteriolar diameters across groups.
 261 N equals number of measured vessel segments. P values were obtained using ANOVA and post-hoc tests.
 262 Abbreviations: DM = diabetes mellitus, DR = diabetic retinopathy, NPDR = non-proliferative diabetic
 263 retinopathy.

264 **Table 4.** Summary of Venular Blood Velocity by Vessel Diameter Groups, Comparing Healthy
 265 Controls, Diabetes without Retinopathy, and Non-proliferative Diabetic Retinopathy

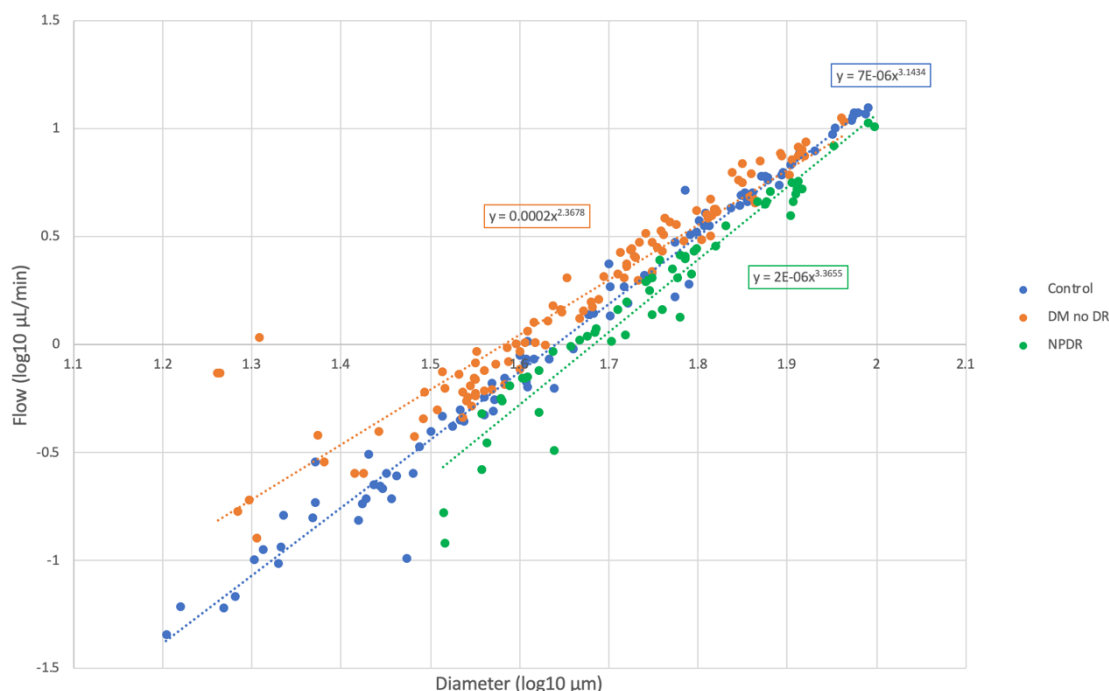
	Control mm/sec (n=39)	DM no DR mm/sec (n=31)	NPDR mm/sec (n=9)	ANOVA P	Control vs DM no DR P	Control vs NPDR P	DM no DR vs NPDR P
< 30µm (n=24)	3.60–8.32, 5.75 (16)	7.56–13.79, 10.09 (8)	n/a	0.000			
31–50µm (n=32)	7.13–13.58, 9.40 (12)	8.29–17.75, 11.51 (15)	3.21–9.05, 5.98 (5)	0.000	0.066	0.026	0.000
> 50µm (n=23)	14.47–25.05, 18.84 (11)	14.43–26.86, 19.45 (8)	7.81–14.29, 9.95 (4)	0.001	0.930	0.001	0.001

266 Blood velocity, expressed as range in mm/sec, mean (n), comparing different venular diameters across groups.
 267 N equals number of measured vessel segments. P values were obtained using ANOVA and post-hoc tests.

268 Abbreviations: DM = diabetes mellitus, DR = diabetic retinopathy, NPDR = non-proliferative diabetic
 269 retinopathy.

270 3.4 Comparison of blood flow across groups

271 Blood flow increased with vessel diameter for all subject groups, as shown on a log-log scale
 272 (Figure 3). Regression coefficients (r) for this relationship were 0.991 for controls, 0.947 for DM
 273 without DR and 0.969 for NPDR eyes. One-way ANOVA showed a statistically significant difference
 274 in mean flow in smaller vessels (up to 60µm), when comparing the three groups (Table 5). Eyes with
 275 DM without DR had significantly higher flow than controls and NPDR in vessels up to 60µm. NPDR
 276 eyes had flow significantly lower than DM no DR in vessels up to 60µm and lower than controls in
 277 vessels greater than 60µm. Blood flow was significantly different in arteries up to 60µm and veins up
 278 to 30µm, when comparing the three groups (Table 6 and Table 7).



279

280 **Figure 3.** Log-log Scale of Blood Flow in Arterioles and Venules by Vessel Diameter, Comparing
 281 Healthy Controls, Diabetes without Retinopathy, and Non-proliferative Diabetic Retinopathy. The
 282 exponent for blood flow as a function of diameter varied about a cubic relation depending on the
 283 patient group. Linear regression coefficients (r) were 0.991 for controls, 0.947 for DM without DR and
 284 0.969 for NPDR eyes. Abbreviations: DM = diabetes mellitus, DR = diabetic retinopathy, NPDR = non-
 285 proliferative diabetic retinopathy.

286 **Table 5.** Summary of Blood Flow in Arterioles and Venules by Vessel Diameter Groups, Comparing
 287 Healthy Controls, Diabetes without Retinopathy, and Non-proliferative Diabetic Retinopathy

	Control µL/min (n=94)	DM no DR µL/min (n=110)	NPDR µL/min (n=56)	ANOVA P	Control vs DM no DR P	Control vs NPDR P	DM no DR vs NPDR P
< 30µm (n=34)	0.05–0.31, 0.16 (23)	0.13–1.07, 0.42 (11)	n/a	0.019			
31–40µm (n=62)	0.25–1.04, 0.58 (20)	0.37–1.16, 0.70 (31)	0.12–0.71, 0.48 (11)	0.004	0.084	0.347	0.005
41–60µm (n=75)	0.62–2.95, 1.59 (15)	0.99–3.85, 2.13 (36)	0.32–2.59, 1.43 (24)	0.000	0.007	0.777	0.007

> 61 (n=89)	1.91–12.44, 6.50 (36)	3.05–11.12, 6.03 (32)	1.91–10.65, 4.86 (21)	0.061	0.719	0.049	0.224
----------------	--------------------------	--------------------------	--------------------------	-------	-------	-------	-------

288 Blood flow, expressed as range in $\mu\text{L}/\text{min}$, mean (n), comparing different vessel diameters across groups. N
 289 equals number of measured vessel segments. *P*-values were obtained using ANOVA and post-hoc tests.
 290 Abbreviations: DM = diabetes mellitus, DR = diabetic retinopathy, NPDR = non-proliferative diabetic
 291 retinopathy.

292 **Table 6.** Summary of Arteriolar Blood Flow by Vessel Diameter Groups, Comparing Healthy
 293 Controls, Diabetes without Retinopathy, and Non-proliferative Diabetic Retinopathy

	Control $\mu\text{L}/\text{min}$ (n=55)	DM no DR $\mu\text{L}/\text{min}$ (n=79)	NPDR $\mu\text{L}/\text{min}$ (n=47)	ANOVA <i>P</i>	Control vs DM no DR <i>P</i>	Control vs NPDR <i>P</i>	DM no DR vs NPDR <i>P</i>
< 30 μm (n=13)	0.06–0.29, 0.16 (9)	0.13–0.40, 0.30 (4)	n/a	0.032			
31–40 μm (n=34)	0.40–0.85, 0.60 (9)	0.45–1.02, 0.73 (18)	0.12–0.71, 0.50 (7)	0.031	0.244	0.570	0.032
41–60 μm (n=57)	0.85–2.95, 1.65 (9)	1.02–3.85, 2.33 (28)	0.48–2.59, 1.51 (20)	0.001	0.051	0.872	0.001
> 60 μm (n=77)	1.91–12.44, 6.68 (13)	3.20–11.12, 6.02 (14)	2.1–10.65, 4.96 (10)	0.068	0.578	0.054	0.314

294 Blood flow, expressed as range in $\mu\text{L}/\text{min}$, mean (n), comparing different arteriolar diameters across groups. N
 295 equals number of measured vessel segments. *P* values were obtained using ANOVA and post-hoc tests.
 296 Abbreviations: DM = diabetes mellitus, DR = diabetic retinopathy, NPDR = non-proliferative diabetic
 297 retinopathy.

298 **Table 7.** Summary of Venular Blood Flow by Vessel Diameter Groups, Comparing Healthy Controls,
 299 Diabetes without Retinopathy, and Non-proliferative Diabetic Retinopathy

	Control $\mu\text{L}/\text{min}$ (n=39)	DM no DR $\mu\text{L}/\text{min}$ (n=31)	NPDR $\mu\text{L}/\text{min}$ (n=9)	ANOVA <i>P</i>	Control vs DM no DR <i>P</i>	Control vs NPDR <i>P</i>	DM no DR vs NPDR <i>P</i>
< 30 μm (n=24)	0.05–0.33, 0.18 (16)	0.17–1.07, 0.47 (8)	n/a	0.043			
31–50 μm (n=32)	7.13–13.58, 9.40 (12)	8.29–17.75, 11.51 (15)	3.21–9.05, 5.98 (5)	0.059	0.542	0.246	0.048
> 50 μm (n=23)	1.86–11.62, 4.80 (11)	1.99–7.68, 3.85 (8)	1.10–2.87, 1.67 (4)	0.119	0.693	0.100	0.337

300 Blood flow, expressed as range in $\mu\text{L}/\text{min}$, mean (n), comparing different venular diameters across groups. N
 301 equals number of measured vessel segments. *P* values were obtained using ANOVA and post-hoc tests.
 302 Abbreviations: DM = diabetes mellitus, DR = diabetic retinopathy, NPDR = non-proliferative diabetic
 303 retinopathy.

304 3.5 Relationship between Velocity and Flow on AOSLO and Capillary Density on OCTA

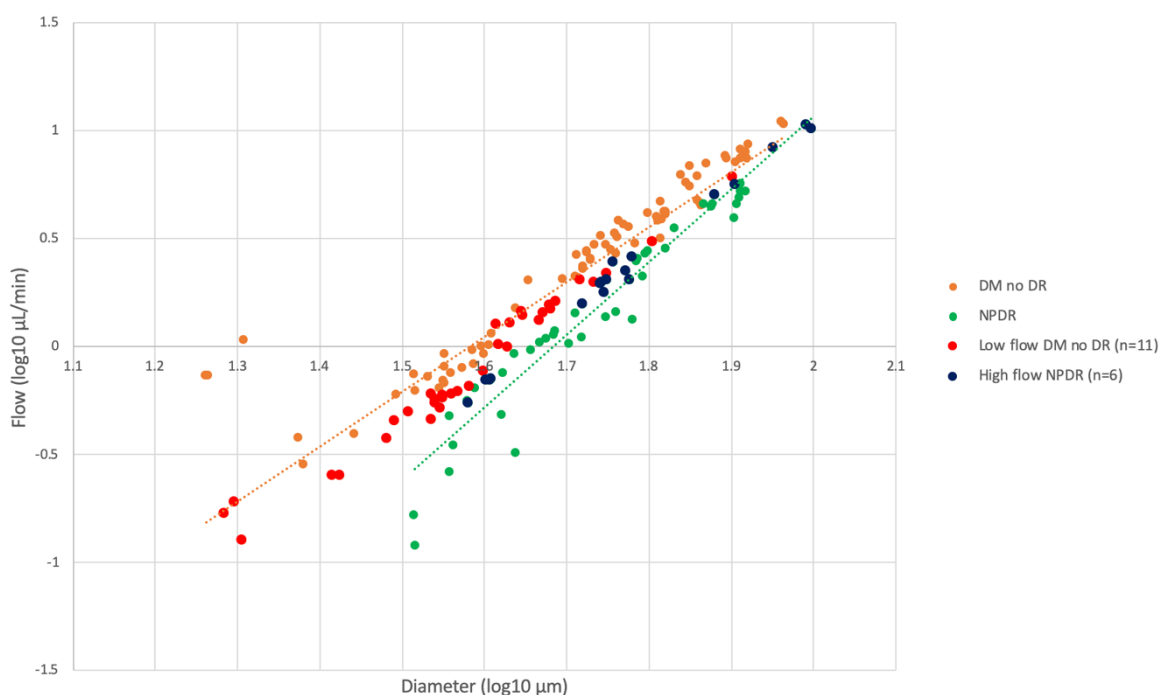
305 In order to better understand the variations in flow across groups, we examined the vessels that
 306 were outliers in flow for each group, defined as being more than one standard deviation (SD) away
 307 from the mean for a specific diameter in a disease group. We determined the relevant eyes and
 308 examined their OCTA vessel density. In the DM no DR group, 13 eyes (13 subjects) had the lowest
 309 flow measurements (0.13–6.11 $\mu\text{L}/\text{min}$), while 8 eyes (8 subjects) had the highest flow measurements
 310 in the NPDR group (0.55–10.65 $\mu\text{L}/\text{min}$). Two eyes from each group were excluded due to poor OCTA
 311 scan quality, leaving 11 “low flow” DM no DR and 6 “high flow” NPDR eyes for further analysis
 312 (**Figure 4**). Independent *t*-tests showed no significant difference between the “low flow” DM with no
 313 DR and the “high flow” NPDR groups when comparing their OCTA parafoveal densities and clinical

314 characteristics (Table 8). The 11 “low flow” DM no DR eyes had significantly lower mean full retina
 315 density than the remaining DM no DR group (53.81 vs 57.02; $P=0.021$) (Figure 4). The 6 “high flow”
 316 NPDR eyes had higher mean full retina density compared to the remaining NPDR group (55.28 vs
 317 53.00), however this difference was not significant ($P=0.497$).

318 **Table 8.** Demographics and Clinical Measurements Comparing Low Flow Diabetes without
 319 Retinopathy and High Flow Non-proliferative Diabetic Retinopathy Eyes

	DM no DR (n=11)	NPDR (n=6)	P
Parafoveal vessel density (%)			
SCP, mean ± SD	43.03 ± 4.98	43.70 ± 3.61	0.252
DCP, mean ± SD	50.71 ± 4.72	46.43 ± 3.17	0.417
Full retina, mean ± SD	53.81 ± 4.59	55.28 ± 1.95	0.123
OCTA SSI, mean ± SD	67.27 ± 3.77	69.83 ± 8.42	0.020
DM type			0.627
Type 1, n (%)	6 (55%)	3 (50%)	
Type 2, n (%)	5 (45%)	3 (50%)	
Disease duration, y, mean ± SD	10.87 ± 8.98	13.33 ± 8.02	0.624
HbA1c, mean ± SD	7.80 ± 2.34	6.77 ± 0.65	0.072
Age, mean ± SD	42.91 ± 16.22	40.17 ± 8.59	0.152

320 Abbreviations: DM = diabetes mellitus, DR = diabetic retinopathy, NPDR = non-proliferative diabetic
 321 retinopathy, SCP = superficial capillary plexus, DCP = deep capillary plexus, SD = standard deviation. P-value
 322 represents independent t-test or Chi-square test between DM without DR and NPDR.



323 **Figure 4.** Log-log Scale Comparison of Blood Flow and Diameter with OCT Vessel Density, Comparing
 324 Diabetes without Retinopathy and Non-proliferative Diabetic Retinopathy. Graph highlighting the
 325 distribution of the “high” and “low flow” outliers as described in the text. Abbreviations: DM no DR =
 326 diabetes mellitus with no diabetic retinopathy, NPDR = non-proliferative diabetic retinopathy.
 327

328 **3.6 Flow measurement precision**

329 To confirm the accuracy of the blood flow measurement, we quantified the total flow in vessels
 330 before and after a bifurcation in each of the three patient groups. The calculated time-averaged blood
 331 flow rate before and after the bifurcations were consistent with physical expectations (Table 9) [43].

332 **Table 9.** Summary of Blood Flow at a Vessel Bifurcation in Healthy Controls, Diabetes without
 333 Diabetic Retinopathy, and Non-proliferative Diabetic Retinopathy

Flow ($\mu\text{L}/\text{min}$)	Healthy control	DM without DR	NPDR
Daughter vessel 1	2.08	0.25	0.93
Daughter vessel 2	3.96	0.37	0.97
Parent vessel	6.03	0.61	1.98

334 4. Discussion

335 Using AOSLO XT imaging, we found that blood flow in eyes with DM without DR was
 336 significantly higher than controls, contrasting with significantly decreased flow in eyes with NPDR.
 337 For blood velocities, the trends were similar, showing statistical significance especially in smaller
 338 vessels. Our results distinguish velocity and flow changes in eyes with DM without DR from mild
 339 NPDR, which had not been possible in previous studies [13,15,16,18,20,23,44]. Using LDV,
 340 researchers found increased retinal blood flow and higher variance of flow in DM no DR compared
 341 to controls [15]. Wang et al. used Doppler OCT and found that eyes with DM no DR had total retinal
 342 blood flow within the normal range, although these eyes had significantly higher flow relative to
 343 PDR [26,45]. One potential explanation for this discrepancy between studies could be explained by
 344 our finding that small vessels ($<60\mu\text{m}$) show the most significant differences in flow in eyes with DM
 345 no DR. Using AOSLO allowed us to reveal these differences as we were able to measure absolute
 346 blood flow across a wider range of vessel diameters (15–100 μm) than previously possible using other
 347 techniques.

348 Our results suggest that during the early stages of diabetes, before the appearance of clinical
 349 retinopathy, there is an increase in retinal blood velocity and blood flow, as observed in the DM
 350 without DR group. This increase in flow, along with increased shear rate, could trigger cumulative
 351 endothelial damage in these eyes [46]. Over time, this damage may ultimately result in capillary
 352 closure, decreased retinal vessel density and ultimately to decreased velocity and flow as seen in eyes
 353 with mild NPDR in our study. To better understand the relationship between flow and vessel density
 354 during the transition from no DR to mild NPDR, we compared OCTA-derived measures of vessel
 355 density to the flow results. While blood flow was elevated in eyes with DM without DR and
 356 decreased in NPDR, we identified a subgroup of vessels that were intermediate between the two
 357 groups (**Figure 4**). We focused on eyes in the DM with no DR group that were 1 SD below the group
 358 means (“low flow”) and NPDR eyes that were higher than the population means (“high flow”). We
 359 found that the 11 “low flow” DM no DR eyes had significantly lower full retina vessel density than
 360 the remaining DM no DR group, while the 6 “high flow” NPDR eyes had higher full retina vessel
 361 density compared to the remaining NPDR group, though not significant. The non-significant
 362 difference in the high flow NPDR group could be attributable to the relatively smaller sample size of
 363 the NPDR eyes. More interestingly, we found that these “low flow” no DR eyes had similar diabetes
 364 duration and OCTA measurements to the “high flow” NPDR, suggesting they may represent a
 365 transitional state and that these eyes are potentially at risk for imminent clinical progression (**Table**
 366 **8**). The overall trend of this dataset suggests that changes in blood flow and vessel density reflect
 367 vascular remodeling and a gradual process of transition to clinically evident retinopathy. This is
 368 consistent with our previously reported finding of significantly increased retinal blood flow and
 369 decreased OCTA vessel density at the superficial capillary plexus (SCP) prior to the onset of clinical
 370 DR [47,48]. It is possible that the increased capillary flow is a compensatory mechanism in these eyes
 371 that enables them to meet the metabolic needs of the retina in the setting of decreased capillary
 372 density which may explain why these eyes do not show clinical retinopathy. It is then possible that
 373 when this compensatory flow mechanism reaches its limit and is no longer able to compensate for
 374 the continued capillary loss, that the clinical manifestations of DR appear along with further decline
 375 in flow and velocity. It remains unclear whether one of these parameters (flow vs. vascular density)
 376 changes prior to the other and drives the vascular pathology. This question can only be answered by
 377 longitudinal, large scale, multimodal AOSLO and OCTA studies.

378 The relationship between vessel diameter and flow is described by Murray's law of branching
379 vasculature, which predicts a cubic relationship [49]. In close agreement, we found that in normal
380 control eyes the mean blood flow varied with vessel diameter in a near cubic relationship (for power
381 fit, exponent=3.15, **Figure 3**). The fitting exponent for DM without DR deviated from this relationship
382 (exponent=2.37) and was lower than controls. The fitting exponent for NPDR was different than DM
383 without DR (exponent=3.37) and was higher than controls. Deviations from Murray's law in the
384 retinal circulation have been seen previously, and are suggested to be related to the Fåhræus-
385 Lindqvist effect, which takes into account the change in blood viscosity by vessel diameter as opposed
386 to the assumption of constant viscosity independent of diameter by Murray [50]. Our findings add
387 further evidence to the notion that changes in blood viscosity and vessel properties, such as rigidity
388 and diameter, may result in deviations from Murray's law in pathologic situations [51]. Diabetes is
389 known to increase blood viscosity and vessel rigidity due to intimal wall thickening [6], resulting in
390 an increased fitting exponent, which we found in the NPDR group. The decrease in the fitting
391 exponent seen in DM with no DR is interesting because it suggests that physiological factors other
392 than viscosity and vessel rigidity could play a role in this group of subjects.

393 The strengths of our study include AOSLO XT imaging, which uniquely allowed us to non-
394 invasively measure absolute blood velocity and flow across a wider diameter range compared to
395 previously used imaging techniques. Because of the video rate acquisition, we were able to capture
396 and average changes occurring over the cardiac cycle. We also acknowledge several limitations of
397 our study. One limitation is that we used the minimum and maximum velocities to determine an
398 average velocity rather than analyzing sequential images to study the pulsatile dynamic changes in
399 velocity. Image acquisition is intensive, requires trained personnel, and currently precludes the
400 routine implementation of this approach in a clinical environment. In addition, the analysis is time
401 consuming and may benefit from automated software tools. Another limitation is the relatively
402 modest sample size of patients with mild NPDR, a limitation of our tertiary retina referral practice
403 and our strict inclusion criteria of treatment-naïve eyes without macular edema. Due to the inflexible
404 orientation of the AOSLO scanner, we were also limited to imaging vessels that were aligned with
405 the direction of scanning. Another limitation is the sensitivity of the system to ocular saccades, which
406 blur the XT image precluding measurements. Although current developments are underway to
407 correct for blur related to eye motion, these have only recently been demonstrated in mice [52]. We
408 were unable to capture vessel diameters <31µm in NPDR eyes, and thereby unable to measure
409 velocity and flow in the smallest capillaries. This was related to the greater number of blurred XT
410 images in these smaller vessels, likely due to relatively unstable fixation in the NPDR group. Finally,
411 we did not measure or account for blood pressure or glucose level at the time of imaging, which may
412 potentially contribute to measurement variability [11,53,54].

413 5. Conclusions

414 In conclusion, using AOSLO we found that patients with DM without DR had significantly
415 increased retinal vascular velocity and flow, while those with mild NPDR had significantly decreased
416 measurements compared to controls. Future directions include long-term follow up of the subjects
417 with DM without DR to study whether the decline in retinal blood velocity and flow could predict
418 the onset of retinopathy in an individual subject and whether the rate of decreased flow can predict
419 the rate of future progression of DR. Further studies to compare AOSLO-based capillary velocity and
420 flow with OCTA-measured parameters such as parafoveal densities may provide additional insights
421 into the nature of the interactions between retinal blood flow, capillary loss and retinopathy
422 progression.

423 **Author Contributions:** conceptualization, A.A.F.; methodology, C.A.P., A.G., S.A.B., and A.A.F.; software,
424 S.A.B.; validation, C.A.P., H.E.L. and J.S.; formal analysis, C.A.P. and H.E.L.; investigation, A.A.F.; resources,
425 A.A.F.; data curation, C.A.P. and H.E.L.; writing—original draft preparation, C.A.P.; writing—review and
426 editing, C.A.P., R.A.L., S.A.B. and A.A.F.; visualization, A.A.F.; supervision, A.A.F.; project administration,
427 H.E.L.; funding acquisition, A.A.F.

428 **Funding:** This research was funded by the National Institutes of Health 1DP3DK108248 (AAF). The funding
429 agencies had no role in study design, data collection and analysis, decision to publish, or preparation of the
430 manuscript.

431 **Acknowledgments:** Research instrument and software support by Boston Micromachines Corporation,
432 Cambridge, Massachusetts, USA and research instrument support by Optovue, Inc. The funding agencies had
433 no role in study design, data collection and analysis, decision to publish, or preparation of the manuscript.

434 **Conflicts of Interest:** The authors declare no conflict of interest.

435 References

- 436 1. Boyle, J.P.; Thompson, T.J.; Gregg, E.W.; Barker, L.E.; Williamson, D.F. Projection of the year 2050
437 burden of diabetes in the US adult population: dynamic modeling of incidence, mortality, and
438 prediabetes prevalence. *Popul Health Metr* **2010**, *8*, 29, doi:10.1186/1478-7954-8-29.
- 439 2. Antonetti, D.A.; Klein, R.; Gardner, T.W. Diabetic retinopathy. *N Engl J Med* **2012**, *366*, 1227-1239,
440 doi:10.1056/NEJMra1005073.
- 441 3. Yau, J.W.; Rogers, S.L.; Kawasaki, R.; Lamoureux, E.L.; Kowalski, J.W.; Bek, T.; Chen, S.J.; Dekker, J.M.;
442 Fletcher, A.; Grauslund, J., et al. Global prevalence and major risk factors of diabetic retinopathy.
443 *Diabetes Care* **2012**, *35*, 556-564, doi:10.2337/dc11-1909.
- 444 4. Cho, Y.I.; Mooney, M.P.; Cho, D.J. Hemorheological disorders in diabetes mellitus. *J Diabetes Sci Technol*
445 **2008**, *2*, 1130-1138, doi:10.1177/193229680800200622.
- 446 5. Kohner, E.M.; Hamilton, A.M.; Saunders, S.J.; Sutcliffe, B.A.; Bulpitt, C.J. The retinal blood flow in
447 diabetes. *Diabetologia* **1975**, *11*, 27-33.
- 448 6. McMillan, D.E. Deterioration of the microcirculation in diabetes. *Diabetes* **1975**, *24*, 944-957.
- 449 7. McMillan, D.E. The effect of diabetes on blood flow properties. *Diabetes* **1983**, *32 Suppl 2*, 56-63.
- 450 8. Schmetterer, L.; Wolzt, M. Ocular blood flow and associated functional deviations in diabetic
451 retinopathy. *Diabetologia* **1999**, *42*, 387-405, doi:10.1007/s001250051171.
- 452 9. Kohner, E.M. The problems of retinal blood flow in diabetes. *Diabetes* **1976**, *25*, 839-844.
- 453 10. Cunha-Vaz, J.G.; Fonseca, J.R.; de Abreu, J.R.; Lima, J.J. Studies on retinal blood flow. II. Diabetic
454 retinopathy. *Arch Ophthalmol* **1978**, *96*, 809-811.
- 455 11. Bursell, S.E.; Clermont, A.C.; Kinsley, B.T.; Simonsen, D.C.; Aiello, L.M.; Wolpert, H.A. Retinal blood
456 flow changes in patients with insulin-dependent diabetes mellitus and no diabetic retinopathy. *Invest*
457 *Ophthalmol Vis Sci* **1996**, *37*, 886-897.
- 458 12. Clermont, A.C.; Aiello, L.P.; Mori, F.; Aiello, L.M.; Bursell, S.E. Vascular endothelial growth factor and
459 severity of nonproliferative diabetic retinopathy mediate retinal hemodynamics in vivo: a potential role
460 for vascular endothelial growth factor in the progression of nonproliferative diabetic retinopathy. *Am*
461 *J Ophthalmol* **1997**, *124*, 433-446.
- 462 13. Grunwald, J.E.; Riva, C.E.; Sinclair, S.H.; Brucker, A.J.; Petrig, B.L. Laser Doppler velocimetry study of
463 retinal circulation in diabetes mellitus. *Arch Ophthalmol* **1986**, *104*, 991-996.
- 464 14. Grunwald, J.E.; Brucker, A.J.; Grunwald, S.E.; Riva, C.E. Retinal hemodynamics in proliferative diabetic
465 retinopathy. A laser Doppler velocimetry study. *Invest Ophthalmol Vis Sci* **1993**, *34*, 66-71.
- 466 15. Grunwald, J.E.; DuPont, J.; Riva, C.E. Retinal haemodynamics in patients with early diabetes mellitus.
467 *Br J Ophthalmol* **1996**, *80*, 327-331.
- 468 16. Feke, G.T.; Buzney, S.M.; Ogasawara, H.; Fujio, N.; Goger, D.G.; Spack, N.P.; Gabbay, K.H. Retinal
469 circulatory abnormalities in type 1 diabetes. *Invest Ophthalmol Vis Sci* **1994**, *35*, 2968-2975.
- 470 17. Konno, S.; Feke, G.T.; Yoshida, A.; Fujio, N.; Goger, D.G.; Buzney, S.M. Retinal blood flow changes in
471 type I diabetes. A long-term follow-up study. *Invest Ophthalmol Vis Sci* **1996**, *37*, 1140-1148.

- 472 18. Patel, V.; Rassam, S.; Newsom, R.; Wiek, J.; Kohner, E. Retinal blood flow in diabetic retinopathy. *BMJ*
473 **1992**, *305*, 678-683.
- 474 19. Cuypers, M.H.; Kasanardjo, J.S.; Polak, B.C. Retinal blood flow changes in diabetic retinopathy
475 measured with the Heidelberg scanning laser Doppler flowmeter. *Graefes Arch Clin Exp Ophthalmol*
476 **2000**, *238*, 935-941.
- 477 20. Grunwald, J.E.; Riva, C.E.; Baine, J.; Brucker, A.J. Total retinal volumetric blood flow rate in diabetic
478 patients with poor glycemic control. *Invest Ophthalmol Vis Sci* **1992**, *33*, 356-363.
- 479 21. Mendivil, A.; Cuartero, V.; Mendivil, M.P. Ocular blood flow velocities in patients with proliferative
480 diabetic retinopathy and healthy volunteers: a prospective study. *Br J Ophthalmol* **1995**, *79*, 413-416.
- 481 22. Goebel, W.; Lieb, W.E.; Ho, A.; Sergott, R.C.; Farhoumand, R.; Grehn, F. Color Doppler imaging: a new
482 technique to assess orbital blood flow in patients with diabetic retinopathy. *Invest Ophthalmol Vis Sci*
483 **1995**, *36*, 864-870.
- 484 23. MacKinnon, J.R.; McKillop, G.; O'Brien, C.; Swa, K.; Butt, Z.; Nelson, P. Colour Doppler imaging of the
485 ocular circulation in diabetic retinopathy. *Acta Ophthalmol Scand* **2000**, *78*, 386-389.
- 486 24. Dimitrova, G.; Kato, S.; Yamashita, H.; Tamaki, Y.; Nagahara, M.; Fukushima, H.; Kitano, S. Relation
487 between retrobulbar circulation and progression of diabetic retinopathy. *Br J Ophthalmol* **2003**, *87*, 622-
488 625.
- 489 25. Wang, Y.; Bower, B.A.; Izatt, J.A.; Tan, O.; Huang, D. In vivo total retinal blood flow measurement by
490 Fourier domain Doppler optical coherence tomography. *J Biomed Opt* **2007**, *12*, 041215,
491 doi:10.1117/1.2772871.
- 492 26. Wang, Y.; Fawzi, A.A.; Varma, R.; Sadun, A.A.; Zhang, X.; Tan, O.; Izatt, J.A.; Huang, D. Pilot study of
493 optical coherence tomography measurement of retinal blood flow in retinal and optic nerve diseases.
494 *Invest Ophthalmol Vis Sci* **2011**, *52*, 840-845, doi:10.1167/iovs.10-5985.
- 495 27. Lee, B.; Novais, E.A.; Waheed, N.K.; Adhi, M.; de Carlo, T.E.; Cole, E.D.; Moulton, E.M.; Choi, W.; Lane,
496 M.; Bauman, C.R., et al. En Face Doppler Optical Coherence Tomography Measurement of Total Retinal
497 Blood Flow in Diabetic Retinopathy and Diabetic Macular Edema. *JAMA Ophthalmol* **2017**, *135*, 244-251,
498 doi:10.1001/jamaophthalmol.2016.5774.
- 499 28. Srinivas, S.; Tan, O.; Nittala, M.G.; Wu, J.L.; Fawzi, A.A.; Huang, D.; Sadda, S.R. Assessment of Retinal
500 Blood Flow in Diabetic Retinopathy Using Doppler Fourier-Domain Optical Coherence Tomography.
501 *Retina* **2017**, *37*, 2001-2007, doi:10.1097/IAE.0000000000001479.
- 502 29. Lee, J.C.; Wong, B.J.; Tan, O.; Srinivas, S.; Sadda, S.R.; Huang, D.; Fawzi, A.A. Pilot study of Doppler
503 optical coherence tomography of retinal blood flow following laser photocoagulation in poorly
504 controlled diabetic patients. *Invest Ophthalmol Vis Sci* **2013**, *54*, 6104-6111, doi:10.1167/iovs.13-12255.
- 505 30. Pinhas, A.; Dubow, M.; Shah, N.; Chui, T.Y.; Scoles, D.; Sulai, Y.N.; Weitz, R.; Walsh, J.B.; Carroll, J.;
506 Dubra, A., et al. In vivo imaging of human retinal microvasculature using adaptive optics scanning
507 light ophthalmoscope fluorescein angiography. *Biomed Opt Express* **2013**, *4*, 1305-1317,
508 doi:10.1364/BOE.4.001305.
- 509 31. Burns SA, E.A., Sapoznik KA, Warner RL, Gast TJ. Adaptive optics imaging of the human retina.
510 *Progress in Retinal and Eye Research* **2019**, *68*, 1-30.
- 511 32. Chui, T.Y.; Gast, T.J.; Burns, S.A. Imaging of vascular wall fine structure in the human retina using
512 adaptive optics scanning laser ophthalmoscopy. *Invest Ophthalmol Vis Sci* **2013**, *54*, 7115-7124,
513 doi:10.1167/iovs.13-13027.

- 514 33. Bedggood, P.; Metha, A. Direct visualization and characterization of erythrocyte flow in human retinal
515 capillaries. *Biomed Opt Express* **2012**, *3*, 3264-3277, doi:10.1364/BOE.3.003264.
- 516 34. Sulai, Y.N.; Scoles, D.; Harvey, Z.; Dubra, A. Visualization of retinal vascular structure and perfusion
517 with a nonconfocal adaptive optics scanning light ophthalmoscope. *J Opt Soc Am A Opt Image Sci Vis*
518 **2014**, *31*, 569-579, doi:10.1364/JOSAA.31.000569.
- 519 35. Zhong, Z.; Petrig, B.L.; Qi, X.; Burns, S.A. In vivo measurement of erythrocyte velocity and retinal blood
520 flow using adaptive optics scanning laser ophthalmoscopy. *Opt Express* **2008**, *16*, 12746-12756.
- 521 36. Zhong, Z.; Song, H.; Chui, T.Y.; Petrig, B.L.; Burns, S.A. Noninvasive measurements and analysis of
522 blood velocity profiles in human retinal vessels. *Invest Ophthalmol Vis Sci* **2011**, *52*, 4151-4157,
523 doi:10.1167/iovs.10-6940.
- 524 37. de Castro A, H.G., Sawides L, Luo T, Burns SA. Rapid high resolution imaging with a dual-channel
525 scanning technique. *Opt Lett*. **2016**, *41*, 1881-1884.
- 526 38. Classification of diabetic retinopathy from fluorescein angiograms. ETDRS report number 11. Early
527 Treatment Diabetic Retinopathy Study Research Group. *Ophthalmology* **1991**, *98*, 807-822.
- 528 39. Grading diabetic retinopathy from stereoscopic color fundus photographs--an extension of the
529 modified Airlie House classification. ETDRS report number 10. Early Treatment Diabetic Retinopathy
530 Study Research Group. *Ophthalmology* **1991**, *98*, 786-806.
- 531 40. Jia, Y.; Tan, O.; Tokayer, J.; Potsaid, B.; Wang, Y.; Liu, J.J.; Kraus, M.F.; Subhash, H.; Fujimoto, J.G.;
532 Hornegger, J., et al. Split-spectrum amplitude-decorrelation angiography with optical coherence
533 tomography. *Opt Express* **2012**, *20*, 4710-4725, doi:10.1364/OE.20.004710.
- 534 41. Asdourian, G.K.; Goldberg, M.F. The angiographic pattern of the peripheral retinal vasculature. *Arch*
535 *Ophthalmol* **1979**, *97*, 2316-2318.
- 536 42. Dubra, A.; Sulai, Y. Reflective afocal broadband adaptive optics scanning ophthalmoscope. *Biomed Opt*
537 *Express* **2011**, *2*, 1757-1768, doi:10.1364/BOE.2.001757.
- 538 43. Sherman, T.F. On connecting large vessels to small. The meaning of Murray's law. *J Gen Physiol* **1981**,
539 *78*, 431-453.
- 540 44. Lorenzi, M.; Feke, G.T.; Cagliero, E.; Pitler, L.; Schaumberg, D.A.; Berisha, F.; Nathan, D.M.; McMeel,
541 J.W. Retinal haemodynamics in individuals with well-controlled type 1 diabetes. *Diabetologia* **2008**, *51*,
542 361-364, doi:10.1007/s00125-007-0872-0.
- 543 45. Wang, Y.; Fawzi, A.; Tan, O.; Gil-Flamer, J.; Huang, D. Retinal blood flow detection in diabetic patients
544 by Doppler Fourier domain optical coherence tomography. *Opt Express* **2009**, *17*, 4061-4073.
- 545 46. Kohner, E.M.; Patel, V.; Rassam, S.M. Role of blood flow and impaired autoregulation in the
546 pathogenesis of diabetic retinopathy. *Diabetes* **1995**, *44*, 603-607.
- 547 47. Onishi, A.C.; Nesper, P.L.; Roberts, P.K.; Moharram, G.A.; Chai, H.; Liu, L.; Jampol, L.M.; Fawzi, A.A.
548 Importance of Considering the Middle Capillary Plexus on OCT Angiography in Diabetic Retinopathy.
549 *Invest Ophthalmol Vis Sci* **2018**, *59*, 2167-2176, doi:10.1167/iovs.17-23304.
- 550 48. Nesper, P.L.; Roberts, P.K.; Onishi, A.C.; Chai, H.; Liu, L.; Jampol, L.M.; Fawzi, A.A. Quantifying
551 Microvascular Abnormalities With Increasing Severity of Diabetic Retinopathy Using Optical
552 Coherence Tomography Angiography. *Invest Ophthalmol Vis Sci* **2017**, *58*, BIO307-BIO315,
553 doi:10.1167/iovs.17-21787.
- 554 49. Murray, C.D. The Physiological Principle of Minimum Work: I. The Vascular System and the Cost of
555 Blood Volume. *Proc Natl Acad Sci U S A* **1926**, *12*, 207-214.
- 556 50. Fåhræus, R.L., T. The Viscosity of the Blood in Narrow Capillary Tubes. *Am J Physio* **1931**, *96*, 562-568.

- 557 51. Luo, T.; Gast, T.J.; Vermeer, T.J.; Burns, S.A. Retinal Vascular Branching in Healthy and Diabetic
558 Subjects. *Invest Ophthalmol Vis Sci* **2017**, *58*, 2685-2694, doi:10.1167/iovs.17-21653.
- 559 52. Joseph, A.; Guevara-Torres, A.; Schallek, J.B. Imaging single-cell blood flow in the smallest to largest
560 vessels in the living retina. 2019; 10.1101/533919.
- 561 53. Grunwald, J.E.; Riva, C.E.; Martin, D.B.; Quint, A.R.; Epstein, P.A. Effect of an insulin-induced decrease
562 in blood glucose on the human diabetic retinal circulation. *Ophthalmology* **1987**, *94*, 1614-1620.
- 563 54. Robinson, F.; Riva, C.E.; Grunwald, J.E.; Petrig, B.L.; Sinclair, S.H. Retinal blood flow autoregulation in
564 response to an acute increase in blood pressure. *Invest Ophthalmol Vis Sci* **1986**, *27*, 722-726.
565



© 2019 by the authors. Submitted for possible open access publication under the terms and conditions of the Creative Commons Attribution (CC BY) license (<http://creativecommons.org/licenses/by/4.0/>).

566